Clinically prevalent mutations in *Mycobacterium tuberculosis* alter propionate metabolism and mediate multidrug tolerance

Supplementary Figures

Table of Contents:

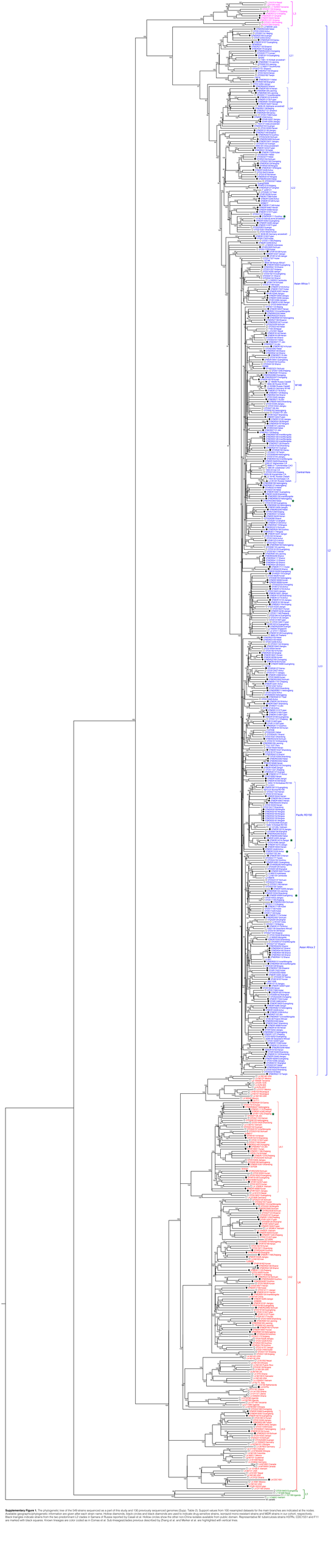

Supplementary Figure 1. The phylogenetic tree of the 549 strains sequenced as a part of this study and 130 previously sequenced genomes (Supp. Table 2). Support values from 100 resampled datasets for the main branches are indicated at the nodes. Available geographic/phylogenetic information are given after each strain name. Hollow diamonds, black circles and black diamonds are used to indicate drug sensitive strains, isoniazid mono-resistant strains and MDR strains in our cohort, respectively. Black triangles indicate strains from the two predominant L2 clades in Samara of Russia reported by Casali et al. Hollow circles show the other non-China isolates available from public domain. Representative M. tuberculosis strains H37Rv, CDC1551 and F11 are marked with black squares. Known lineages are color coded as in Comas et al. Sub-lineages/clades previous described by Zhang et al. and Merker et al. are highlighted with vertical lines.

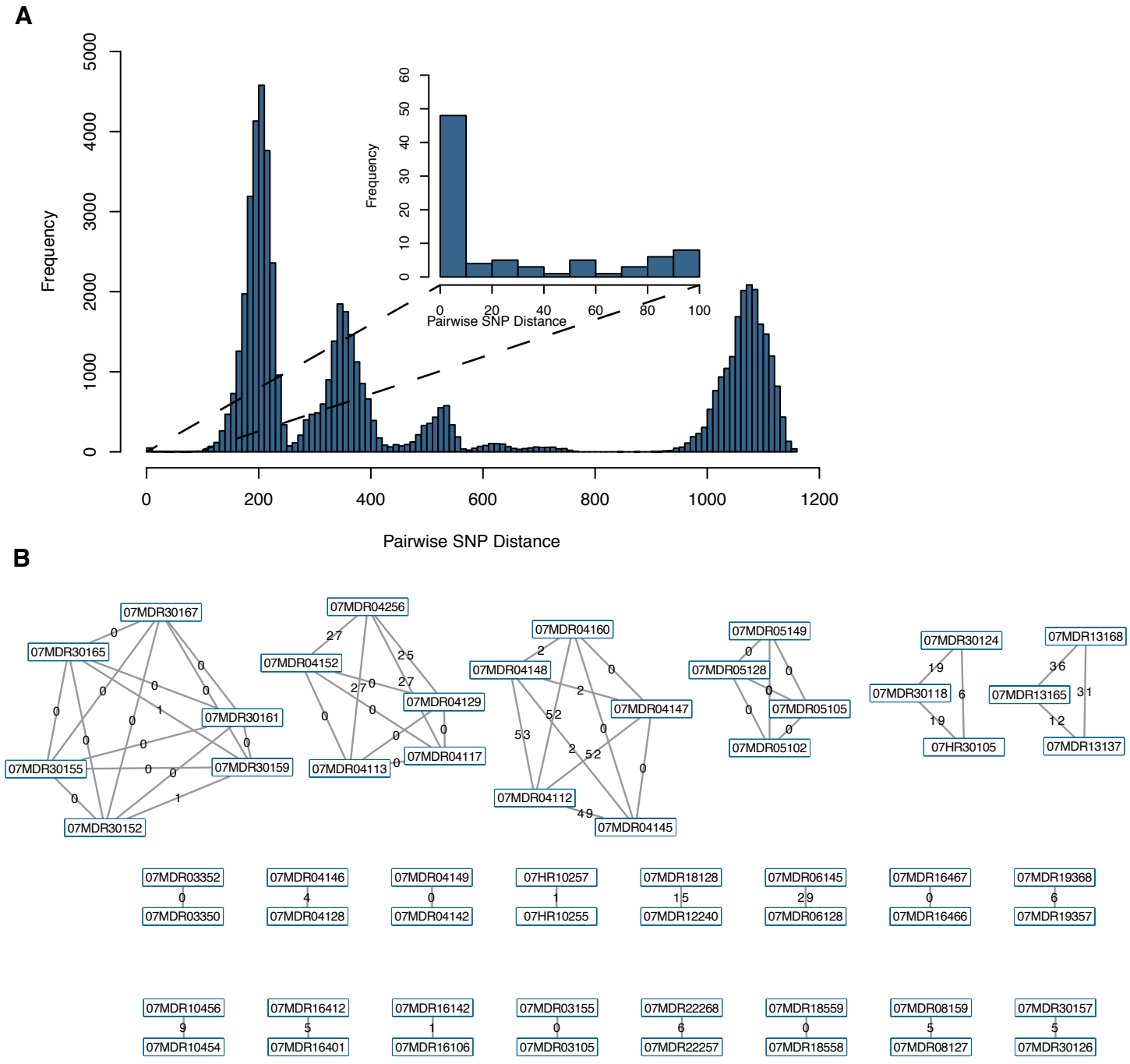

Supplementary Figure 2. Cluster analysis of drug resistant strains. (A) Pairwise SNP distances among all drug resistant isolates. Inset zoomed into the number of pairs with a 100 SNP threshold. (B) Networks of drug resistant clusters showing isolates as nodes and edges as pairwise distances. Isolates included within any cluster also contain the same INH resistance-determining mutation.

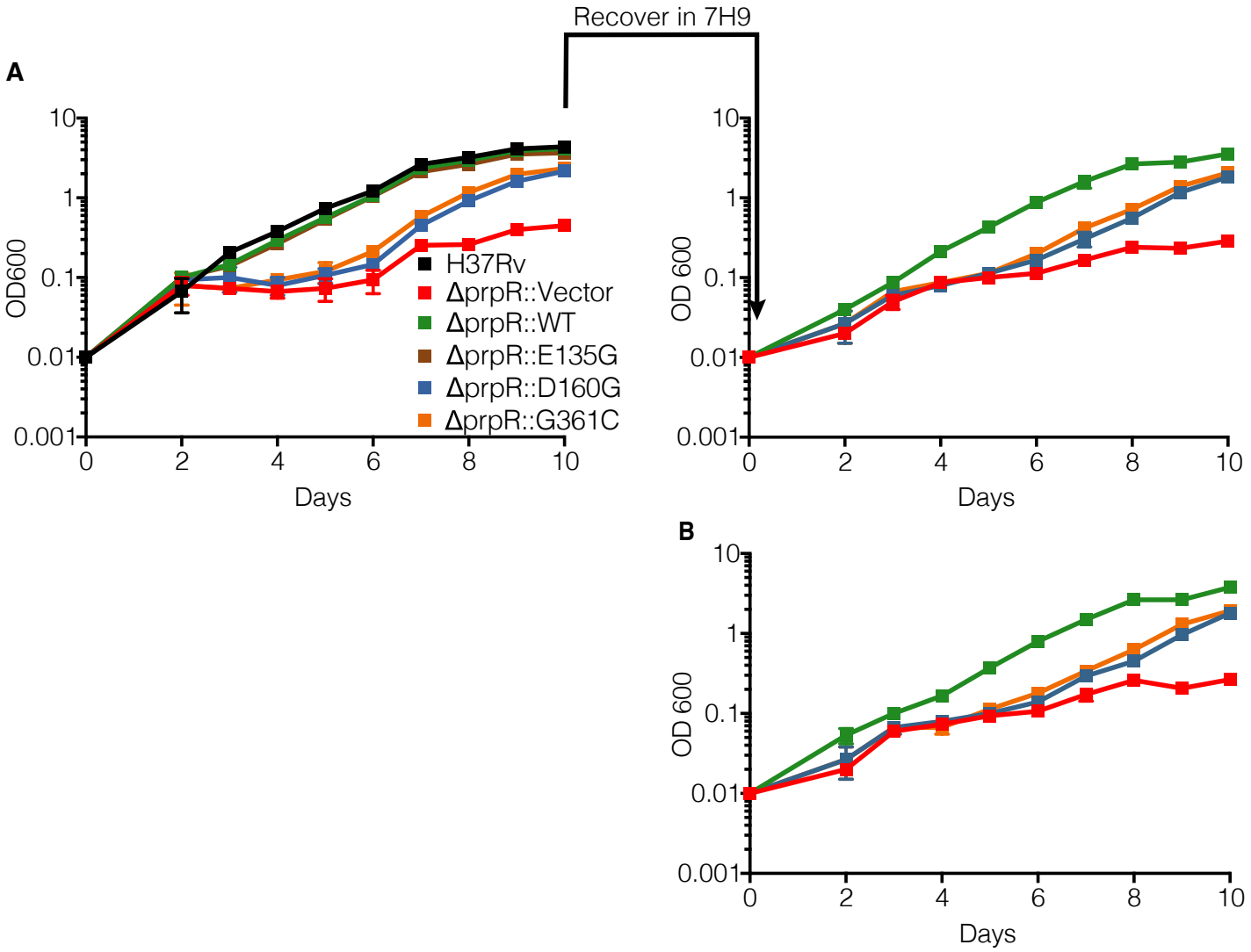

Supplementary Figure 3. Re-growth of prpR mutants after propionate exposure. (A) Strains exposed to propionate were recovered after 10 days of growth, recovered, in 7H9 OADC media for 7 days, and then re-exposed to 7H12 with propionate supplementation. (B) Growth of prpR mutants directly from freezer stocks in 7H12 propionate media performed concurrently with the pre-exposed strains. Data represents the mean and standard deviation of three biological replicates.

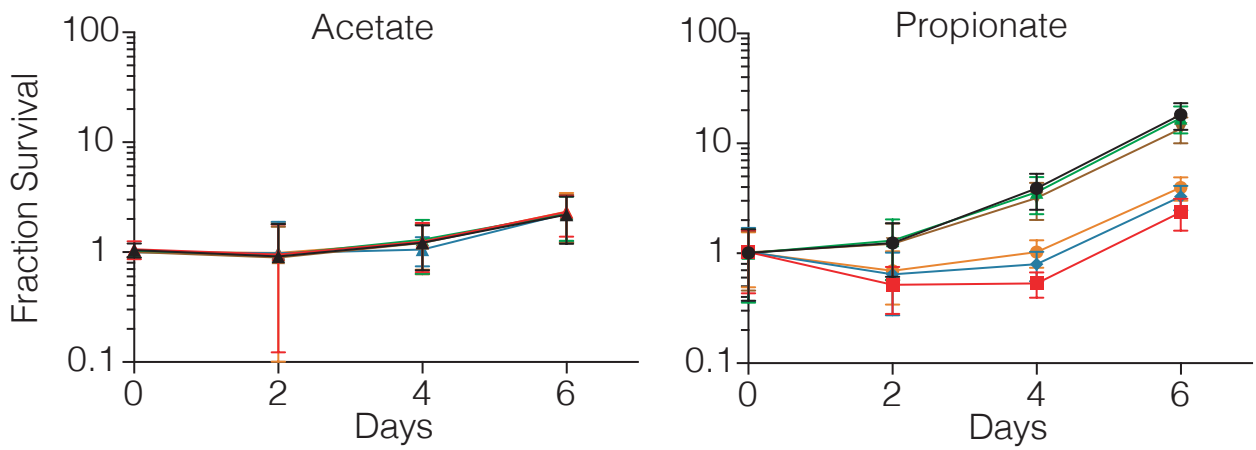

Supplementary Figure 4. Calculated CFU of prpR mutants in no drug controls corresponding to the library format antibiotic treatment depicted in Figure 3D. Data points represent the mean and standard deviation of three biological replicates.

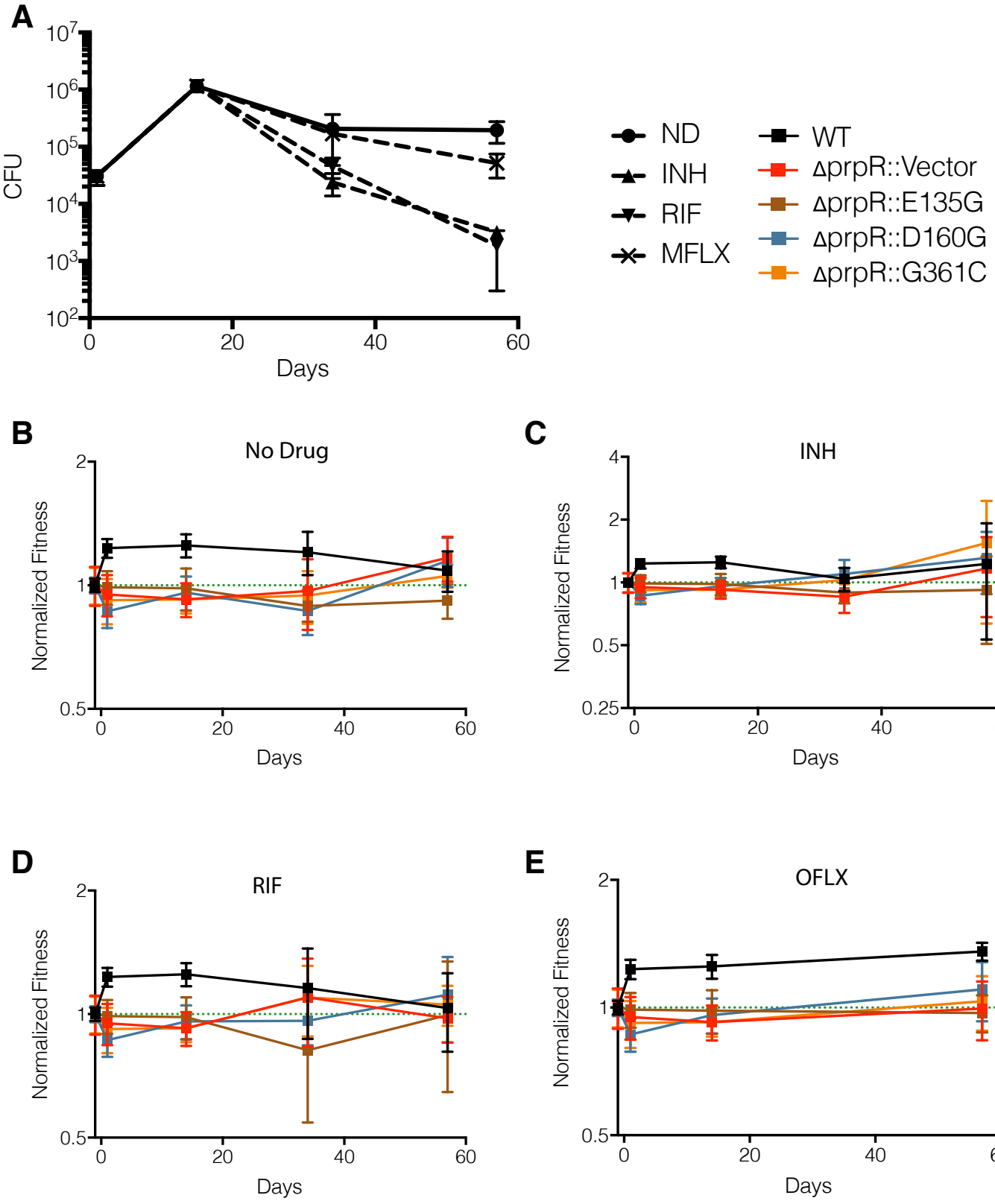

Supplementary Figure 5. The relative abundance of prpR mutants in a mouse model of infection normalized to the input library composition. (A) Infected mice were sacrificed at 1, 14, 34, and 57 days post infection and the bacterial burden was determined by plating serial dilutions of homogenized spleen samples on 7H10 agar. Antibiotic treatment was initiated at 14 days post infection. (B-E) Concurrently with CFU determination, bacteria were recovered, gDNA was extracted from >500 colonies, and the relative abundance of each strain was determined by deep sequencing. The abundance of each strain relative to ΔprpR::WT was measured and normalized to the input library shown as day -1. The CFU and relative abundance measurement depicted is the mean of 5 mice, except the day 1 measurement, which is the mean of 3 mice. Error bars represent standard deviation.

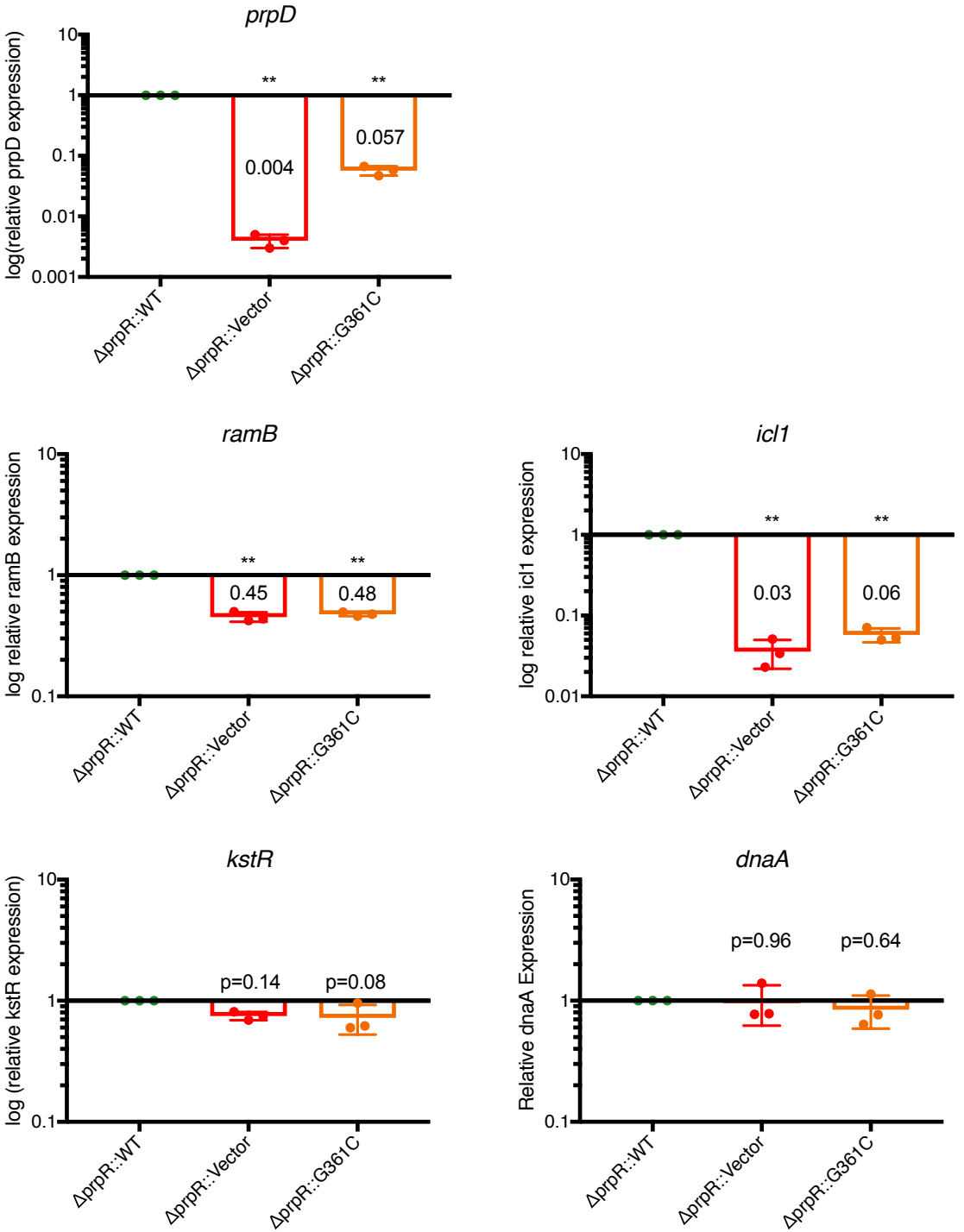

Supplementary Figure 6. Relative expression of a panel of proposed prpR targets measured by qPCR and normalized to sigA expression after two days of growth in 7H12 supplemented with propionate. Fold-expression is normalized to ΔprpR::WT with error bars representing standard deviation and the decimal value of ΔprpR::WT expression annotated within the bar. Significant differences among strains was tested by Tukey's multiple comparisons test after one-way ANOVA. ** signifies $p < 0.001$.

Supplementary Figure 7

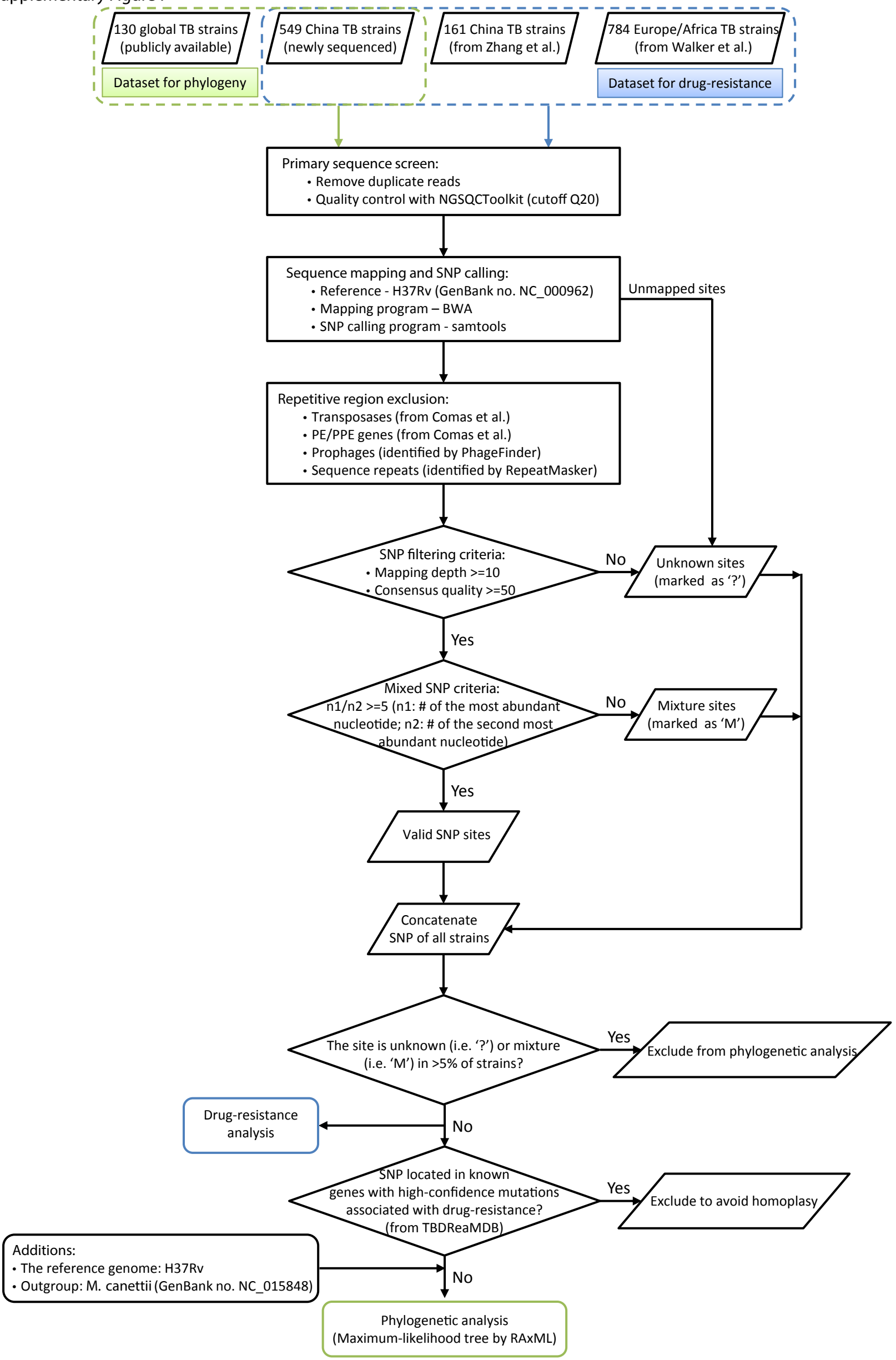

Supplementary Figure 7. A detailed workflow depicting the SNP calling analysis pipeline and filtering scheme for incorporation of data into each analysis.